

# The Relationship of Four Brain Regions to an Information-Processing Model of Numerical Inductive Reasoning Process: An fMRI Study

Xiuqin Jia<sup>1,2</sup> and Peipeng Liang<sup>1,2\*</sup>

<sup>1</sup>Department of Radiology, Xuanwu Hospital, Capital Medical University, Beijing, 100053, China

<sup>2</sup>Beijing Key Lab of MRI and Brain Informatics, Beijing, 100053, China

**Abstract:** The present study relates a four-stage information-processing model of inductive reasoning to four brain regions. We assume that there is a fusiform gyrus region-of-interest (ROI) where a stimulus is visually recognized, a DLPFC ROI where an underlying rule is identified, a caudate ROI where a rule is applied, and a motor ROI where hand movements are programmed during inductive reasoning process. Then, an fMRI experiment was performed to articulate the roles of these four regions. The present study is a 2 (task: rule induction vs. rule application)  $\times$  2 (period length: simple vs. complex)  $\times$  2 (priming effect: prime vs. target) design. As predicted, both the fusiform gyrus ROI and the motor ROI showed no effects of task, period length, and priming effect, and respectively reflected encoding of stimuli and button-pressing response. The DLPFC ROI responded to task and period length, and was confirmed to play a crucial role in rule identification. The caudate showed no effect of task and responded to period length and priming effect, and was verified to be responsible for rule application. The exploratory analysis also demonstrated our assumptions. Thus, the main stream of information-processing in inductive reasoning process can be described by using the four ROIs.

**Keywords:** Dorsolateral Prefrontal Cortex (DLPFC), Functional MRI, Inductive Reasoning, Number Series Completion.

## INTRODUCTION

Inductive reasoning, defined as the process of inferring a general rule from specific instances, underlies many cognitive activities including concept formation, problem solving, learning, scientific discovery [1]. Considered to be at the core of human intelligence [2], inductive reasoning is used not only to acquire new knowledge but also to make the acquired knowledge more readily applicable in new contexts [3]. Although this topic has been extensively studied in logic and psychology [4-5], its neural mechanism is less investigated and understood [6-9].

## NUMBER SERIES COMPLETION: A TYPICAL INDUCTIVE REASONING TASK

Number series completion is a typical inductive reasoning task. For example, given a number series {2, 4, 6, 8, 10}, a general rule ( $X(i+1) = X(i) + 2$ ) which defines the relations among the constituent elements has to be identified and subsequently applied to continue the series. As it is better to balance the background knowledge across participants, the number series completion task has been widely used in psychological studies. For example, Wason *et al.*

(1968) design “2-4-6” tasks to study the testing of hypotheses [10]. Simon and his colleagues [11-13] have used number series completion tasks (or similar tasks, such as alphabet series completion tasks and function-finding tasks) in their studies of scientific discovery and problem solving.

Studies indicate that four basic cognitive components are involved in solving number series completion problems [14-16]. The first component is the encoding of number series. The second component, identification, contains three sub-components: (i) Relations detection, requires scan of the series and generation of a hypothesis about the relation among adjacent elements. Relations between elements are determined by the type of arithmetic operation (*e.g.*, addition/subtraction, multiplication/division, etc.) and the magnitude of the operation involved. (ii) Discovery of periodicity, involves detection of period boundary and structure. Simple series have a period length of 1 (such as {1, 3, 5, 7, 9}, period length=1, rule: +2), while complex series have longer period lengths (such as {2, 4, 3, 5, 4}, period length=2, rule: +2,-1). (iii) Completion of the pattern description, involves identification of the relations between the elements composing a cycle, and then formulation a rule accounts for the sequence both between and within periods. The third component, extrapolation, consists of three sub-components: (i) Detection of answer position; (ii) Isolation of part of the rule; and (iii)

\*Address correspondence to this author at the Xuanwu Hospital, Capital Medical University, 45 Chang Chun Street, Xi Cheng District, Beijing 100053, China.  
E-mail: ppliang1979@gmail.com

Application of this part of the rule in computing the answer. The period length is critical in determining the processing requirements to solve a number series. The simple task (period length=1) is solved through fewer processing stages, and the stages of discovery of periodicity, detection of answer position and isolation of part of the rule do not apply to the simple task. Finally, the fourth component, answer production, is followed.

In their serial behavioral and neuropsychological studies, Delazer and his colleagues have validated the steady priming effect on number series completion tasks [14, 17-18]. The priming effect means that exposure to a piece of information such as a word/object/concept (prime) facilitates its subsequent processing (target) [19]. The priming effect on number series completion tasks opens a new window to explore the neural mechanism of human inductive reasoning.

### STATE-OF-THE-ART OF THE NEURAL CORRELATES OF NUMERICAL INDUCTIVE REASONING

Several brain imaging studies have investigated the neural correlates of inductive reasoning by using normal subjects [7-8, 20-24] and patients [25]. These studies concern the neural correlates of priming effect [24], or the cognitive components of simple number series completion tasks [21], or the strategy effects [20], and or complexity effect [22-23], among which the important role of the (dorsal/lateral) prefrontal cortex (PFC) in inductive reasoning during rule identification was mainly discussed. In the present study, we assume that there is induction-based network responsible for inductive reasoning including a fusiform gyrus region-of-interest (ROI) where a stimulus is visually recognized, a DLPFC ROI where an underlying rule is identified, a caudate ROI where a rule is applied, and a motor ROI where hand movements are programmed. However, the relationship of this inductive reasoning-based network to an information-processing model remains unclear.

### THE FOUR-STAGE INFORMATION-PROCESSING MODEL OF INDUCTIVE REASONING PROCESS

Inductive reasoning process can be partitioned into four stages: encoding, rule identification, rule application, and response. We called it the four-stage information-processing model of inductive reasoning process as shown in Figure 1. When we encounter some instances in the real world, we will firstly encode them, and then try to identify the underlying common

rule, and then validate the rule by applying them to the new instance, finally the answer can be produced. It is noted that the four-stage model is always not sequential but a dynamic and cyclic hypothesis formation and validation process, in which the identified regulation will be revised when the negative instance is met. As abovementioned, the cognitive components of the number series completion task have shown an example of this model.

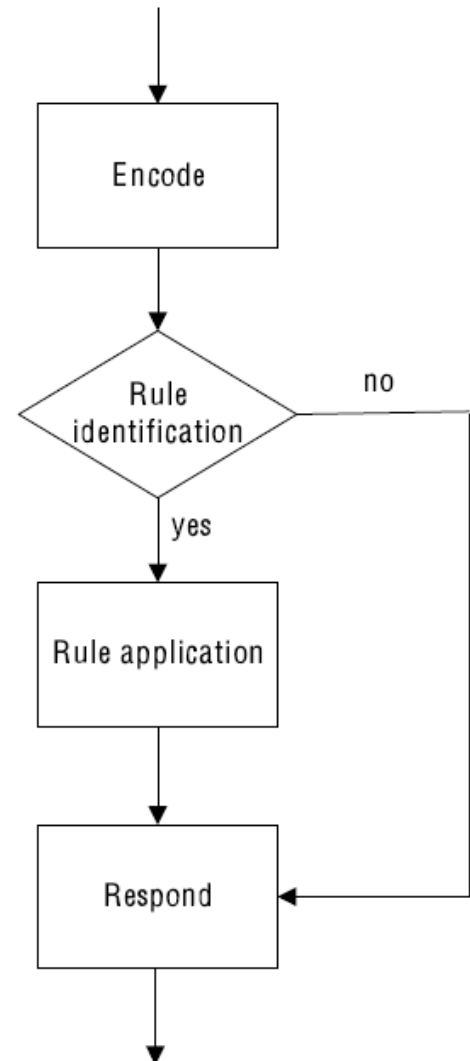


**Figure 1:** The four-stage information-processing model of inductive reasoning process.

The four-stage information-processing model is consistent with the other cognitive models of human inductive reasoning, including Sternberg's cognitive components approach [26-27] and Klauer's training model of inductive reasoning [28-29]. Both Sternberg's and Klauer's model suggest that the identical four cognitive components are common for various inductive reasoning tasks including numerical, verbal,

and figural tasks, although their model is constructed for different goals. Additionally, ACT-R (Adaptive control of Thought - Rational) [30-32], a unified information-processing theory for simulating and understanding human cognition, can also be used to characterize inductive reasoning process. There are a set of modules involved in ACT-R, including identifying objects in the visual field, retrieving information from declarative memory, keeping track of current goals and intentions, controlling the hands and reporting vocally. Thus, the four-stage information-processing model is also congruent with the ACT-R model. However, the four-stage information-processing model just characterizes the inductive reasoning process psychologically. In this article, we will further relate each process of the four-stage model to corresponding brain areas based on fMRI data.

**THE CURRENT STUDY**

The present study primarily aimed to test the associations of these four brain regions to specific information-processing components. Our hypotheses relate these four brain areas to the four-stage information-processing model of inductive reasoning process: the fusiform gyrus ROI may visually encode elements from the screen; the DLPFC ROI may play a critical role in rule identification; the caudate ROI may be responsible for rule application; and the motor ROI may program hand movements to respond. The second focus of present study was to assess the degree to which the recruitment of these four brain areas was left lateralized, especially for the DLPFC ROI. Previous studies of inductive reasoning which reported the left lateralization of the DLPFC adopted sentential tasks [6]. This research would use the numerical task, *i.e.*, number series completion, which might not have the same degree of the left lateralization. We would examine each pair of symmetrical ROIs distributed bilaterally.

Except the rest task, the fundamental design of the experiment was a 2 × 2 × 2 design with task (rule induction vs. rule application), period length (simple vs. complex), and priming effect (prime vs. target). We have the following predictions:

1. The visual ROI would show no effect of lateralization, task, period length and priming effect.
2. The DLPFC ROI would be left lateralized, and show a stronger effect of task and period length.
3. The caudate ROI would show no effect of lateralization, and show an effect of period length and priming effect. The caudate ROI would show no effect of task.
4. The motor ROI would show no effect of lateralization, task, period length and priming effect.

**MATERIALS AND METHODS**

**Subjects**

13 paid healthy students (7 male and 6 female, aged 24.6±2.2, right-handed, normal or corrected-to-normal vision) participated in the experiment. Written informed consent was obtained from each participant and this study was approved by the Ethics committee of Xuanwu Hospital, Capital Medical University.

**Tasks**

The experiment adopted a 2 × 2 × 2 design as shown in Table 1. Additionally, the rest task (*i.e.*, {0, 0, 0, 0, 0}) was also designed as the lowest baseline for all the other experimental tasks. All numbers including answers ranged in 0-99, and only addition and subtraction were employed in the present study. Each number contained in the target task was different from every number in the prime task. The answer of the target task was different from that of the prime task. For

**Table 1: Illustration of the Nine Conditions of Experiment, in which the Four Italic Items Represent the Rules for Application Task**

		Prime		Target	
Induction	Simple		4,6,8,10,12		41,43,45,47,49
	Complex		14,15,18,19,22		22,23,26,27,30
Application	Simple	(+3)	17,20,23,26,29	(+3)	32,35,38,41,44
	Complex	(-1,+2)	28,27,29,28,30	(-1,+2)	53,52,54,53,55
Rest			0,0,0,0,0		

example, the prime and the target had different perceptual features (e.g., {31, 33, 35, 37, 39} vs. {12, 14, 16, 18, 20}), and required different arithmetic computations (prime:  $39 + 2$ , target:  $20 + 2$ ) and different answers (prime: 41, target: 22). Then, totally 200 tasks (20 tasks for each kind of task, and other 20 interferential tasks) were designed.

The period length was used to define simple ( $L=1$ , e.g., {1,3,5,7,9} with rule:  $+2$ ) and complex ( $L=2$ , e.g., {1,3,6,8,11} with rule:  $+2,+3$ ) number series tasks. For simple tasks, the rule magnitudes were set to 3, 4, 6, 7, 8, 9, 12, and 13 (0, 1, 2, 5, 10, 11, 14, 15, 16, 17, 18, and 19 were not used, which was a trade-off between the number of tasks and the experimental time). For complex tasks (e.g., rule  $\pm a, \pm b$ ), we had  $0 < a < 10$  and  $0 < b < 10$ .

### Stimuli Presentation

Number series were presented on the computer screen in white digits in 36 size font against a black background as shown in Figure 2. Stimuli were preceded by a cue of task type for 1.5 s, and followed by a 0.5 s fixation “+” for attention. Then a number series was shown for 13 s. Participants were instructed to press button as quickly as possible after attaining the value followed, and move to the next trial if the stimuli advanced before they could respond. After button-pressing response, participants should orally report the answer within 3 s. Finally a fixation of “+” was presented for 6 s as ISI (Inter-Stimulus Interval). The subjects were instructed to respond as accurately and quickly as possible and to move to the next trial if the stimuli advanced before they could respond.

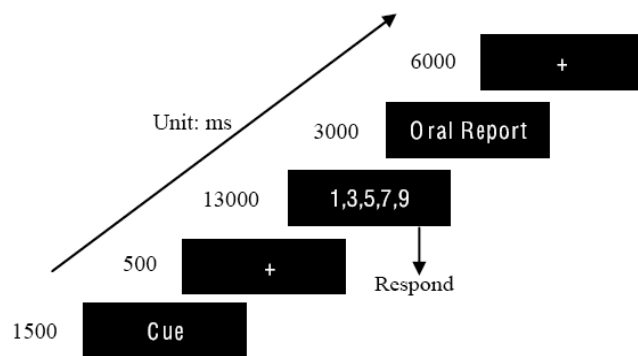


**Figure 2:** The 24 s structure of an fMRI trial in the present study.

The filler between the prime task and the target task was 1. Different kinds of tasks or tasks with different rules acted as fillers for each other. The cues for task types were “Identifying a rule”, “Applying a rule ( $\pm a, \pm b$ )”, and “Rest”, respectively. All tasks were evenly and pseudo-randomly distributed in four sessions. Button-pressing responses were balanced among participants.

### fMRI Data Acquisition

Scanning was performed on Siemens Magnetom Trio Tim 3.0 T system using a standard whole-head coil. Functional data were acquired using a gradient echo planar pulse sequence (TR = 2 s, TE = 31 ms, 30 axial slices,  $3.75 \times 3.75 \times 4.0$  mm<sup>3</sup> voxels, 0.8 mm interslice gap, 90° flip angle,  $64 \times 64$  matrix size in  $240 \times 240$  mm<sup>2</sup> field of view). The imaging sequence was optimized for detection of the BOLD effect including local shimming and 10 s of scanning prior to data collection to allow the MR signal to reach equilibrium. To minimize head motion, bi-temporal pressure pads were employed. The scanner was synchronized with the presentation of every trial.

### Data Processing of fMRI

fMRI data were analyzed using SPM5 (Wellcome Institute of Neurology at University College London, UK. <http://www.fil.ion.ucl.ac.uk/spm>). The first two images were discarded to allow for T1 equilibration effects. The remaining fMRI images were first corrected for within-scan acquisition time differences between slices and then realigned to the first volume to correct for inter-scan head motion (the head movements were  $< 2$  mm and  $< 2^\circ$  in all cases). The realigned functional volumes were spatially normalized to the Montreal Neurological Institute (MNI) space and re-sampled to 3-mm isotropic voxels. The fMRI data were then smoothed with an 8 mm FWHM isotropic Gaussian kernel.

### Pre-Defined ROIs

Based on previous studies four regions-of-interest (ROIs) were defined. Each region was 12 mm wide, 12 mm long, and 12 mm deep (64 voxels per ROI) and was centered at the regions identified in [32-33] and [21]. To explore the laterality of these effects we also looked at pre-defined ROIs in the right hemisphere obtained by just switching the sign of the x coordinate. Thus, our pre-specified ROIs are (as shown in Figure 3):

**Table 2: Areas of Activation.** X, Y, and Z are MNI coordinates. For each contrast, the bracket followed showed the uncorrected voxel-level intensity threshold of  $p$  and the minimum cluster size of contiguous voxels with which the activations were reported: i vs rest ( $p = 0.0001$ , cluster > 20); i vs a ( $p = 0.001$ , cluster > 20); si vs sa ( $p = 0.001$ , cluster > 20); ci vs ca ( $p = 0.001$ , cluster > 20); sip vs sit ( $p = 0.01$ , cluster > 20); cip vs cit ( $p = 0.01$ , cluster > 20); ci vs si ( $p = 0.005$ , cluster > 20); ca vs sa ( $p = 0.005$ , cluster > 20); i, induction; a, application; si, simple induction; sa, simple application; ci, complex induction; ca, complex application

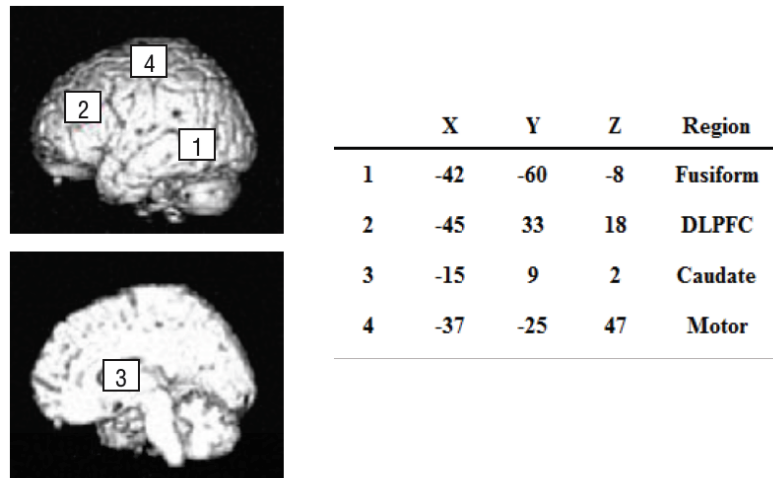
Location (Brodmann Area)	X	Y	Z	T
<b>Induction vs. Rest</b>				
Left inferior frontal gyrus (BA 9)	-42	9	30	17.224
Left middle frontal gyrus (BA 11)	-21	45	-12	5.784
Left medial frontal gyrus (BA 6)	-3	-30	57	6.428
Right inferior frontal gyrus (BA 47)	27	30	-9	9.089
Left medial frontal gyrus (BA 32)	-9	12	48	8.224
Right cingulate gyrus (BA 32)	3	15	39	7.393
Left anterior cingulate (BA 25)	-3	21	0	5.718
Left inferior occipital gyrus (BA 17)	-15	-93	-18	9.747
Left precuneus (BA 31)	-27	-78	18	10.556
Right inferior occipital gyrus (BA 18)	33	-90	-18	12.641
Right middle occipital gyrus (BA 18)	33	-87	0	9.418
Right superior occipital gyrus (BA 39)	33	-72	27	7.016
Left fusiform gyrus (BA 19)	-36	-81	-18	9.879
	-42	-66	-18	9.704
Left inferior parietal lobule (BA 40)	-45	-45	45	7.162
Right inferior parietal lobule (BA 40)	39	-45	48	5.613
Left caudate head	-9	15	6	7.166
	-18	27	6	5.591
Right caudate head	15	18	-3	7.726
Left insula (BA 13)	-30	24	0	6.69
Right insula (BA 13)	30	27	0	7.689
<b>Induction vs. Application</b>				
Left orbital gyrus (BA 11)	-6	45	-21	4.841
Right rectal gyrus (BA 11)	6	39	-21	5.515
Right medial frontal gyrus (BA 11)	6	39	-12	4.966
<b>Simple Induction vs. Simple Application</b>				
Left medial frontal gyrus (BA 11)	-3	42	-15	4.201
Right medial frontal gyrus (BA 11)	6	36	-18	5.147
	3	48	-18	4.737
<b>Complex Induction vs. Complex Application</b>				
Left medial frontal gyrus (BA 10)	-9	51	9	6.092
	-15	39	-12	4.951
Left medial frontal gyrus (BA 11)	-3	51	-18	5.545
	-3	42	-15	4.262
Left inferior frontal gyrus (BA 11)	-24	36	-18	4.647
Right middle frontal gyrus (BA 46)	51	24	27	5.655

Table 2: Continued.

Location (Brodmann Area)	X	Y	Z	T
	45	21	21	5.153
Right inferior frontal gyrus (BA 44)	57	18	15	4.712
Left middle occipital gyrus (BA 18)	-21	-99	0	5.296
Left cuneus (BA 17)	-15	-99	-9	5.152
Left inferior occipital gyrus (BA 17)	-15	-90	-12	4.486
<b>Simple Induction Prime vs. Simple Induction Target</b>				
Left middle frontal gyrus (BA 11)	-39	51	-9	2.702
Left middle frontal gyrus (BA 46)	-54	27	27	2.506
	-54	33	18	2.225
Right middle frontal gyrus (BA 46)	51	27	27	2.746
Left inferior frontal gyrus (BA 44)	-51	15	21	2.103
Right angular gyrus (BA 39)	51	-72	27	3.591
	60	-60	24	2.236
Left inferior parietal lobule (BA 40)	-51	-48	51	3.003
<b>Complex Induction Prime vs. Complex Induction Target</b>				
Right medial frontal gyrus (BA 9)	12	45	27	2.706
Right superior frontal gyrus (BA 8)	15	48	42	2.682
<b>Complex Induction vs. Simple Induction</b>				
Right middle frontal gyrus (BA 46)	57	24	30	5.35
Right inferior frontal gyrus (BA 44)	54	15	12	4.227
Right middle frontal gyrus (BA 9)	51	18	39	4.215
Right middle frontal gyrus (BA 10)	39	60	-9	5.012
Left inferior parietal lobule (BA 40)	-45	-45	57	3.968
	-45	-45	48	3.321
Left postcentral gyrus (BA 40)	-45	-36	51	3.611
Right inferior parietal lobule (BA 40)	39	-54	48	5.461
	42	-45	42	4.837
Right superior parietal lobule (BA 7)	33	-63	45	3.245
Right precuneus (BA 7)	12	-72	42	4.824
Right thalamus	21	-27	0	4.845
	12	-18	9	3.405
Right putamen	27	-21	3	3.198
Left lingual gyrus (BA 17)	-12	-96	-9	5.061
<b>Complex Application vs. Simple Application</b>				
Left superior parietal lobule (BA 7)	-21	-63	60	4.126
Left precuneus (BA 7)	-9	-63	57	3.916
	-18	-63	45	2.924
Right superior parietal lobule (BA 7)	27	-72	51	4.13

1. Fusiform Gyrus: centered at (Talairach coordinates:  $x = \pm 42$ ,  $y = -60$ ,  $z = -8$ ). This area includes parts of Brodmann Area 37.

2. Dorsolateral Prefrontal Cortex (DLPFC): centered at (Talairach coordinates:  $x = \pm 48$ ,  $y = 33$ ,  $z = 18$ ). This area locates in Brodmann Area 46.



**Figure 3:** An illustration of the locations of the four brain regions associated with the four-stage information-processing model. The Talairach coordinates are for the left side. All of these regions are cubes about 4 voxels long, 4 voxels wide, and 4 voxels high.

3. Caudate: centered at (Talairach coordinates:  $x = \pm 15$ ,  $y = 9$ ,  $z = 2$ ). This area locates at the head of the caudate nucleus, part of the basal ganglia.

4. Motor: centered at (Talairach coordinates:  $x = \pm 37$ ,  $y = -25$ ,  $z = 47$ ). This area covers Brodmann Area 3 and 4 at the central sulcus.

The first ROI of the fusiform gyrus locates at the ventral pathway of visual processing. This region may play a critical role in perceptual recognition. The second ROI of DLPFC may be central to inductive reasoning and reflect relation integration. The third ROI locates at the head of the caudate may be associated with action selection (where "action" extends to cognitive as well as physical actions) and represent the firing of productions that unpack the logic involved in solving the number series completion task. The fourth ROI includes parts of both the motor and the sensory cortex may be responsible for programming and execution of hand movements.

Additionally, we also perform exploratory analysis. The hemodynamic response to the presentation of the number series was modeled with the canonical hemodynamic response function and its time derivative employed in SPM5. No scaling was implemented for global effects. The resulting time series across each voxel were high-pass filtered with a cut-off of 128 s to remove section-specific low frequency drifts in the BOLD signal. An auto-regression AR (1) was used to exclude the variance explained by the previous scan. The contrast images for each subject were then used in a random effects analysis to determine what regions

were the most consistently activated across subjects using a one-sample t test. The activations reported survived an uncorrected voxel-level intensity threshold of  $p < 0.005$  with a minimum cluster size of 10 contiguous voxels.

## RESULTS

### Behavioral Performance

Figure 4 shows the behavioral data during fMRI experiment. A three-factor ANOVA (task: rule induction vs. rule application; period length: simple vs. complex; priming effect: prime vs. target) was used in the statistical analysis of the reaction time and percent of correctness. Failure to answer a prime determined the elimination of the corresponding target and vice-versa. For the reaction time, the main effect of task [ $F(1, 12) = 481.228$ ,  $p < 0.005$ ] and period length [ $F(1, 12) = 21.858$ ,  $p < 0.005$ ] were significant while the other effects were not significant. For accuracy, the main effect of task [ $F(1, 12) = 51.858$ ,  $p < 0.005$ ] was significant and the other effects were not significant. Rest was evidently different from the other tasks both for the reaction time and correctness. All participants gained high scores and then there existed a ceiling effect. Thus, correctness was not considered. The results of the reaction time were congruent with expectations. The longer reaction time of rule induction than rule application can be explained by the component of rule identification existed in rule induction while not in rule application. The similar reason can be applied to the main effect of period length. We do not

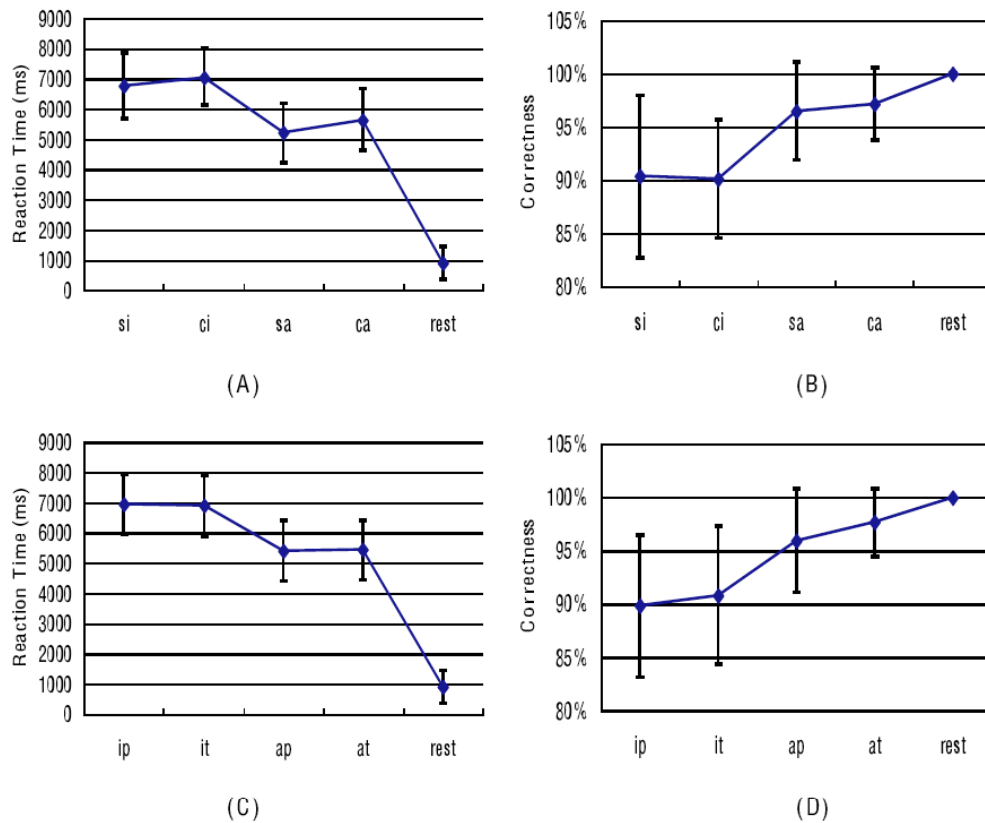


**Figure 4:** Behavioral data during fMRI experiment, including reaction time (A, C) and accuracy (B, D). ip = induction prime; it = induction target; ap = application prime; at = application target; si = simple induction; ci = complex induction; sa = simple application; ca = complex application; i = induction; a = application; rest = rest.

find the significant priming effect from the reaction time, different from the studies of [17-18].

### The Fusiform Gyrus Region

Figure 5 reports the effects of task, period length, and priming effect on the BOLD response both in the left and right fusiform gyrus regions. These curves take as baseline the average of Scans 1 and 2 (before the response begins to rise) and Scan 11 and 12 (by which time it has returned to baseline). Each point is defined as the percent rise above this baseline. We performed an analysis based on the maximum value of the peak during Scans 3-10 rose above the baseline. There was no difference between the left and the right hemisphere. There were also no effects of task, period length, and priming effect. These facts confirm the predictions about this region. The BOLD response in this region seems to reflect visual encoding of number series presented, which is consistent with [34].

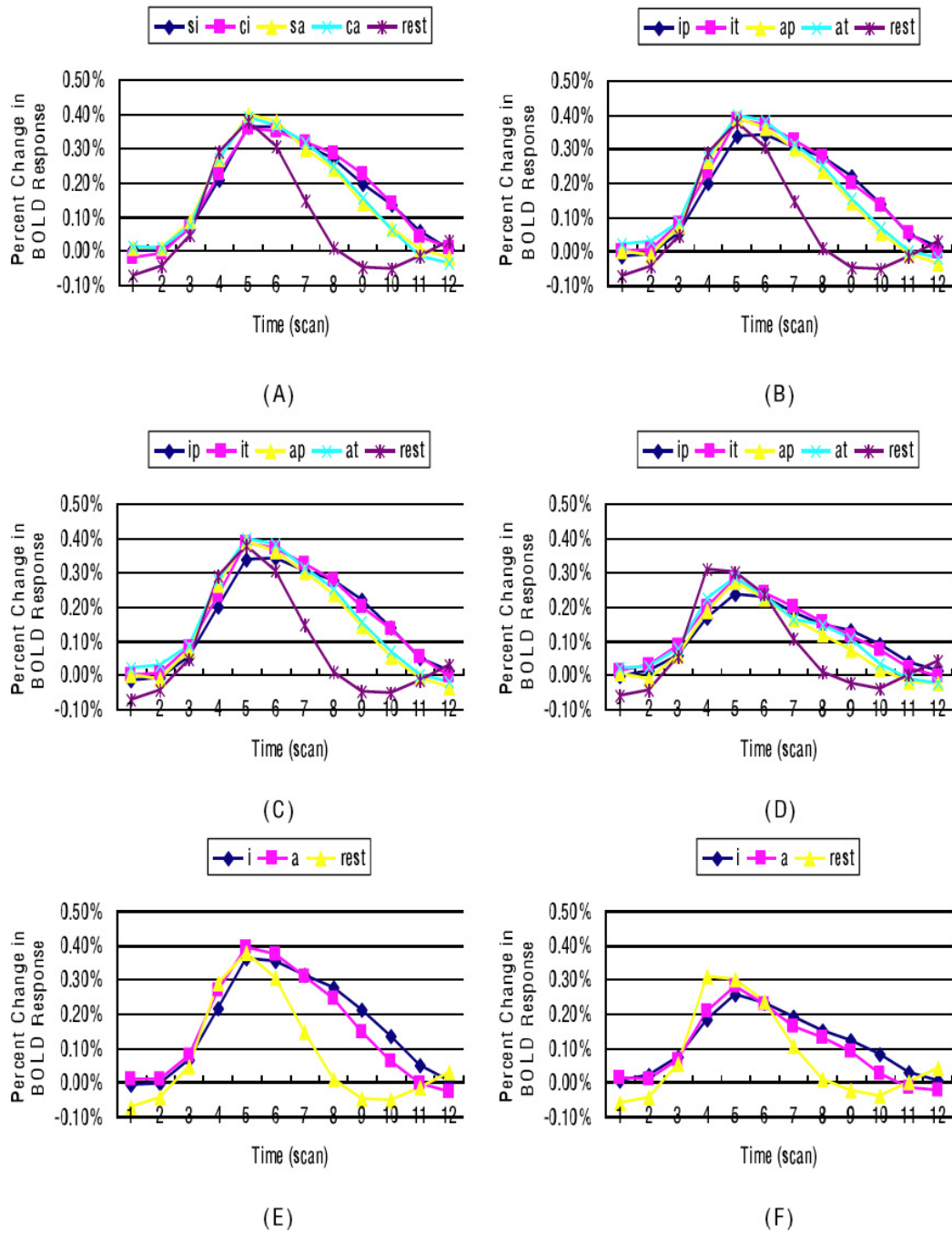
### The DLPFC Region

Figure 6 shows the results for the DLPFC region. It is observed that there has a strongly left lateralization

for the DLPFC ROI. The intensity of BOLD response in the right DLPFC is about half of that in the left DLPFC. This effect is consistent with previous studies [6,8,35-37]. There is a tendency of priming effect for rule induction not for rule application

We have predicted that there would have a stronger effect of task and period length. Statistical analysis demonstrates that the main effects of task [ $F(1, 12) = 13.671$ ;  $p < 0.005$ ] and period length [ $F(1, 12) = 29.259$ ;  $p < 0.005$ ] were significant. The left DLPFC is thought to play a central role in rule identification, which is included in induction while not in application. [32] relate a lateral inferior prefrontal region (Talairach coordinates  $x = -40$ ,  $y = 21$ ,  $z = 21$ ; parts of BA 45 and 46 around inferior frontal sulcus) to controlled retrieval from declarative memory. In fact, the core of rule identification stage is comparison [28-29], while the retrieval of arithmetic knowledge may be concomitant. The retrieval load for simple induction tasks (e.g., identifying a rule: {12, 16, 20, 24, 28}) and complex induction tasks (e.g., identifying a rule: {13, 11, 17, 15, 21}) is identical. Thus, if this area is related to





**Figure 5:** The BOLD responses for the left fusiform gyrus (A,C,E) and right fusiform gyrus (B,D,F). This figure represents the effect between task and period length; C and D represent the effect between task and priming effect; E and F represent the effect of task.

controlled retrieval, there should be no main effects of period length for the induction task. The stronger effect of period length can be explained by the greater demand for comparison in complex induction tasks than simple induction tasks. We also find the evident interaction effect between task and period length [ $F(1, 12) = 6.700; p < 0.05$ ]. Pair-wise comparison showed

that the effect of period length for the induction task (complex induction vs. simple induction, for short, ci vs. si) was more significant than that of the application task (complex application vs. simple application, for short, ca vs. sa), which may further suggest the recruitment of the left DLPFC in inductive reasoning.

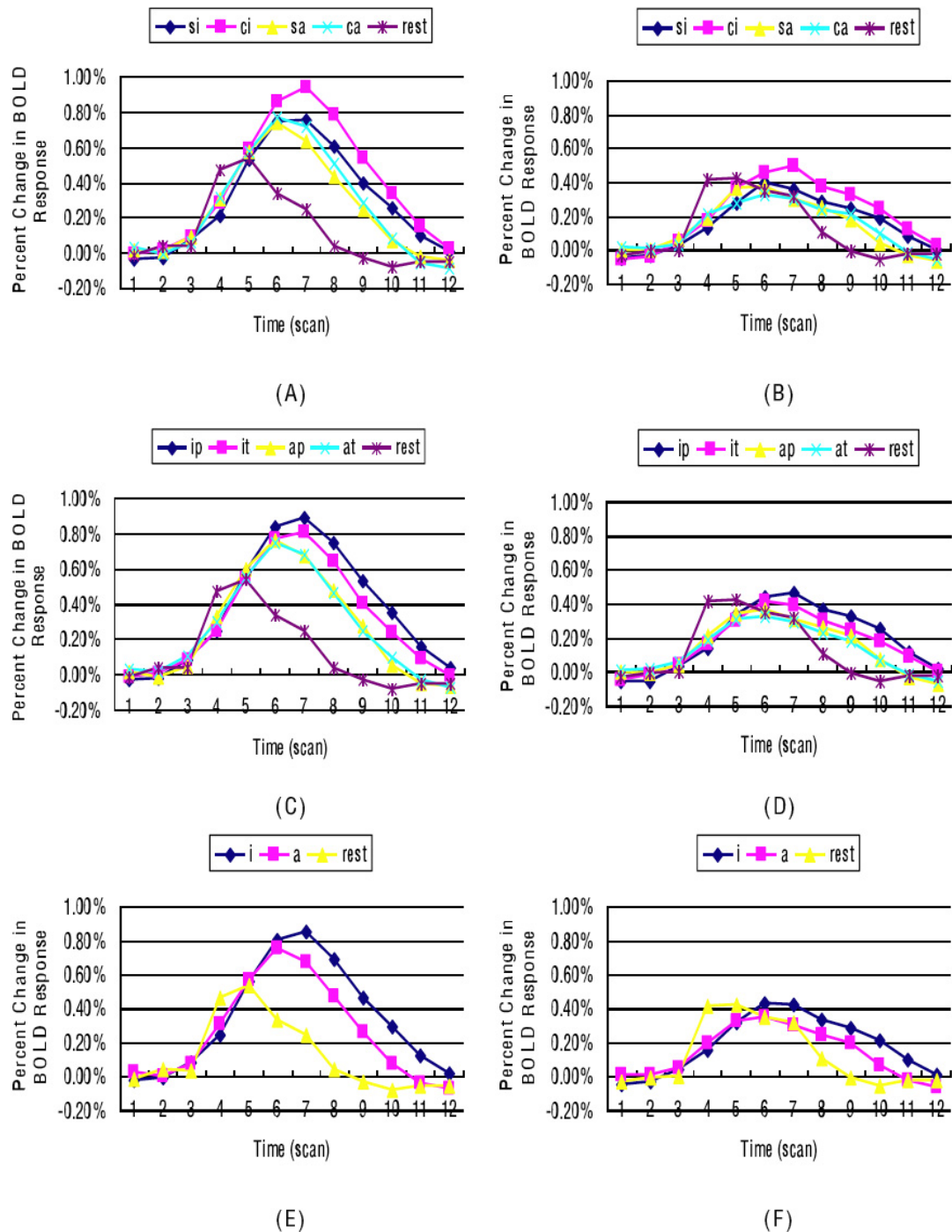


**Figure 6:** The BOLD responses for the left DLPFC (A,C,E) and right DLPFC (B,D,F). A and B represent the effect between task and period length; C and D represent the effect between task and priming effect; E and F represent the effect of task.

### The Caudate Region

Figure 7 displays the average response of the caudate region. The postulations for the caudate nucleus reflect rule application, consistent with ACT-R in which this area is considered to reflect procedural activities. There is no significantly difference between

the left and right caudate, which may indicate that bilateral caudate are both involved in using the rule to attain an answer. There is also no difference among rest, induction and application, while we observe that the rest task rise to peak firstly, and then the application task, and finally the induction task. The fact that three kinds of tasks have the identical signal

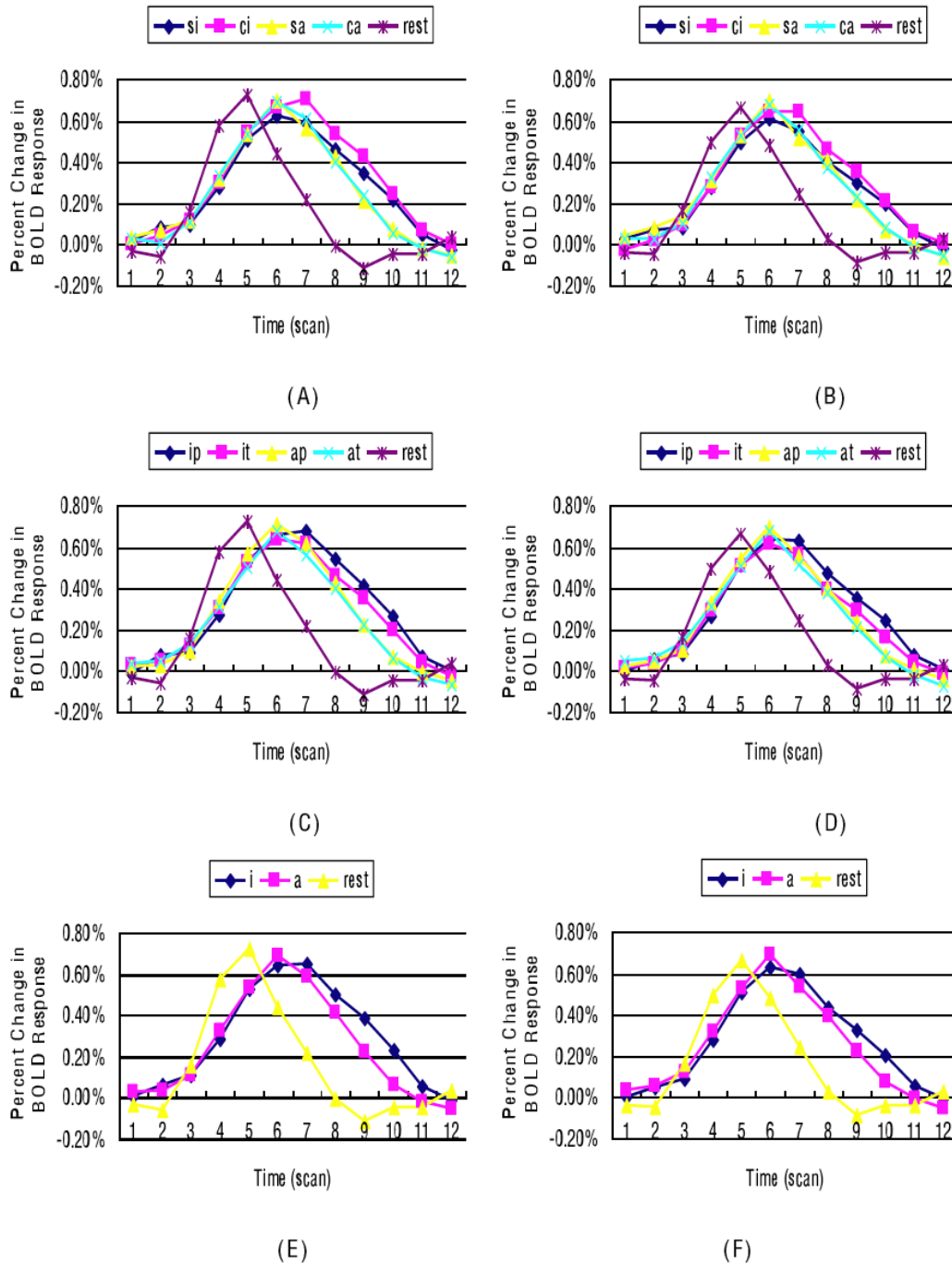


**Figure 7:** The BOLD responses for the left caudate (A,C,E) and right caudate (B,D,F). A and B represent the effect between task and period length; C and D represent the effect between task and priming effect; E and F represent the effect of task.

intensity of BOLD response can be explained by our experimental tasks. The performances of induction, application and rest tasks all contain a kind of “if-then” production rule as instructed. However, the rest task has the lowest task load and can be responded immediately, and the application task can be executed based on given rule, while the induction task should be first inferred of its underlying rule and then the rule can be used. These facts may cause the different latency of

the BOLD responses to rise to their peak for the rest, application and induction task.

Statistical analysis showed the effect of period length [ $F(1, 12) = 5.290; p < 0.05$ ] and priming effect [ $F(1, 12) = 13.744; p < 0.05$ ] for the left caudate and the effect of priming effect [ $F(1, 12) = 4.217; p = 0.062$ ] for the right caudate. The effect of period length in this study may be due to the reason that the activity of the

caudate is associated with the amount of information productions are relying [38]. The experimental design in this study allowed us to exclude the facilitation of perceptual processes, arithmetic fact retrieval, and verbal output as sources of potential facilitation in answering targets. Thus, the fact that the prime task has the same rule with the corresponding target task

can account for the lower BOLD response in the target task than the prime task.

### The Motor Region

Figure 8 gives the average response of the left and right motor regions. This area showed no effect of

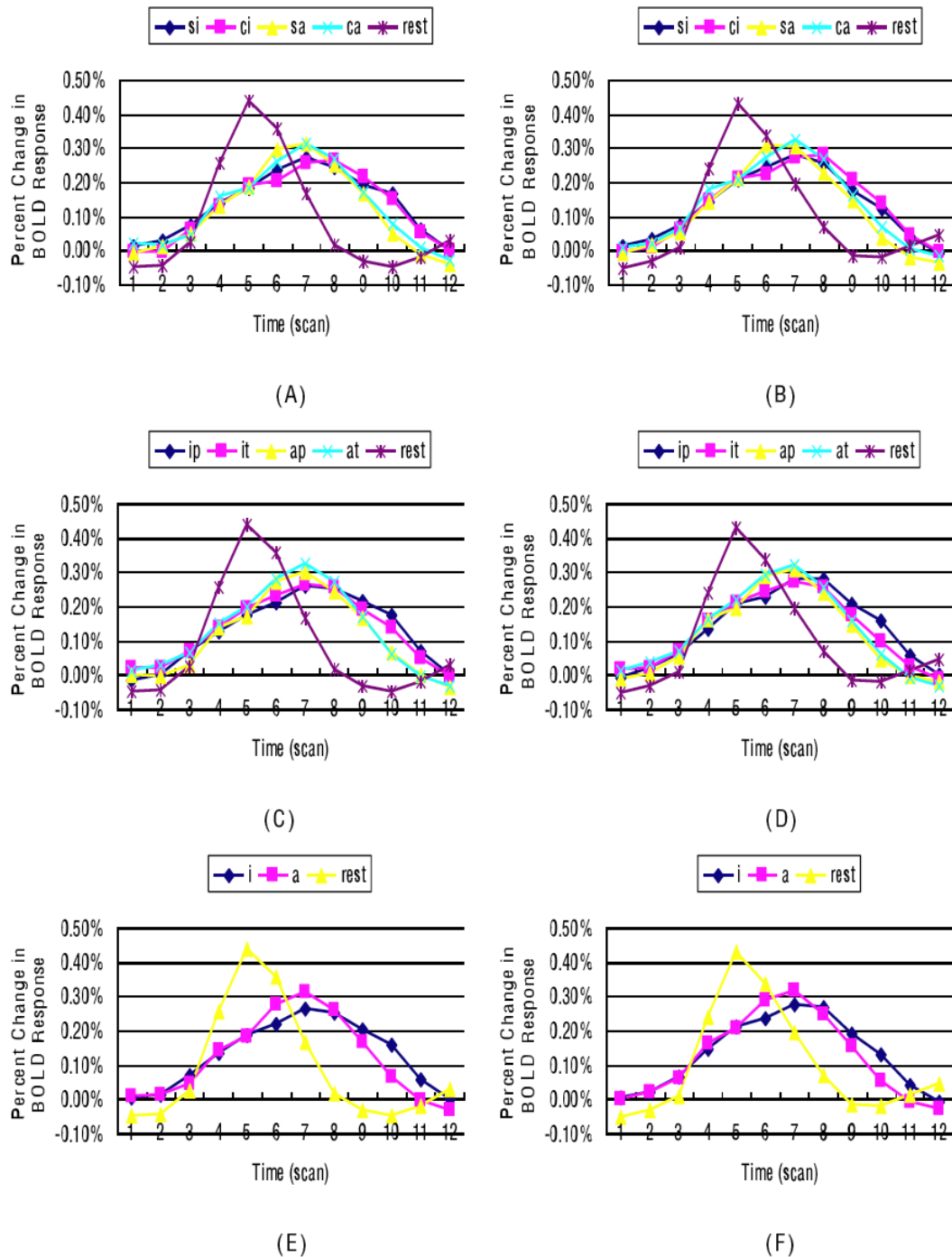


**Figure 8:** The BOLD responses for the left motor region (A,C,E) and right motor region (B,D,F). These two figures represent the effect between task and period length; C and D represent the effect between task and priming effect; E and F represent the effect of task.

lateralization, task, period length and priming effect. For each kind of task, participants should press button to respond, and button-pressing responses were balanced between participants. What is surprise to us is the significant BOLD response of the rest task, and a slight higher for the application task, as compared to the induction task. In combination with participants' reports after scanning, we inferred that these facts may have relation to different mental sets when facing experimental tasks with different (cognitive) difficulties. Many participants reported that they always had a sense of "relaxation" when meeting relatively easy tasks, and often overexert themselves when pressing the button. However, we have been performing the corresponding experiment to further observe this area.

### Exploratory Imaging Analysis

Exploratory analysis as shown in Figure **S1** was conducted to examine whether our confirmatory analysis missed any important brain regions. Table **2** summarizes the regions shown to have significant effects. Examining the comparison of induction vs. rest (i vs. rest) revealed that induction was associated with activation in the left DLPFC (BA 9), left anterior prefrontal cortex (BA 11), left medial frontal gyrus (BA 6), right inferior frontal gyrus (BA 47), bilateral cingulate gyrus (BA 32, 25), bilateral occipital gyrus (BA 17, 18), left fusiform gyrus (BA 19), bilateral inferior parietal lobule (BA 40), bilateral caudate head, and bilateral insula (BA 13). Induction vs. application (i vs. a) mainly activated bilateral anterior prefrontal cortex (BA 11).

The comparison of simple induction vs. simple application (si vs. sa) mainly indicated the activation of bilateral anterior prefrontal gyrus (BA 11). The comparison of complex induction vs. complex application (ci vs. ca) activated left anterior prefrontal gyrus (BA 10, 11), right middle frontal gyrus (BA 46), right inferior frontal gyrus (BA 44), left occipital cortex (BA 17, 18). Compared with simple tasks, complex task also recruited right prefrontal gyrus and left occipital cortex.

The comparison of simple induction prime vs. simple induction target (sip vs. sit) showed the activation in left anterior prefrontal cortex (BA 11), bilateral DLPFC (BA 46), left inferior frontal gyrus (BA 44), right angular gyrus (BA 39) and left inferior parietal lobule (BA 40). The comparison of complex induction prime vs. complex induction target (cip vs. cit) activated right prefrontal gyrus (BA 8, 9). Compared with facilitation in simple induction task, complex induction

task activated more areas in right prefrontal gyrus.

The comparison of complex induction vs. simple induction (ci vs. si) recruited the regions including right DLPFC (BA 9, 46), right inferior frontal gyrus (BA 44), right anterior prefrontal cortex (BA 10), bilateral inferior parietal lobule (BA 40), right superior parietal lobule (BA 7), right thalamus, right putamen, and left lingual gyrus (BA 17). While the comparison of complex application vs. simple application (ca vs. sa) mainly activated the areas in bilateral superior parietal lobule (BA 7).

These facts have demonstrated our predictions of the four ROIs (fusiform gyrus, DLPFC, caudate; while motor area is subtracted). Besides the predefined regions, the exploratory analysis also found some other areas for induction. These are bilateral anterior cingulate gyrus (ACC), bilateral anterior prefrontal cortex (APFC), bilateral occipital gyrus, bilateral inferior parietal lobule (IPL), bilateral insula. ACC has been related to cognitive control [39-40], and this area has been included in some information-processing models such as ACT-R [32]. The bilateral occipital gyrus may be activated during the encoding period and presumably reflects visual examination of the stimulus trying to solve the problem [34]. The bilateral IPL in this study may be linked to number processing including calculation and comparison, as has been widely studied [41-42]. The insula in this study may participate in processes relevant to working memory, which is consistent with the inference that the insula is sensitive to working memory load [43-44]. Bilateral APFC in this study (as shown in Figure **S2**) has also been reported to be associated with evaluation of self-generated information [35,45] and rule induction [46]. For the left APFC in this study, statistical analysis showed that the main effect of task [ $F(1, 12) = 21.581; p < 0.01$ ] was significant, and the interaction effect between task and period length [ $F(1, 12) = 8.798; p < 0.05$ ] was also significant. Pair-wise comparison showed that the effect of period length was only applied to the induction task. For the right APFC, all the effects were not significant. Thus, these evidences may imply the role of the left APFC in inductive reasoning.

Based on components analysis, a region would be more responsible for rule identification if it survives in ci vs. si than ca vs. sa, and a region would be more responsible for rule application if it survives in ca vs. sa than ci vs. si. Thus, directly comparing ci vs. si with ca vs. sa would be helpful to identify the different roles of different regions. Compared with ca vs. sa, ci vs. si

mainly activated DLPFC, APFC, and IPL. DLPFC region has been examined in ROI analysis, and APFC has been reported in previous sections. The BOLD response of the IPL region is shown in Figure S3 (A, B). Statistical analysis showed that the main effect of period length for the left IPL ( $F(1, 12) = 11.058, p < 0.01$ ) was significant, while the interaction effect of task and period length was significant for both the left IPL ( $F(1, 12) = 11.077, p < 0.01$ ) and the right IPL ( $F(1, 12) = 9.597, p < 0.01$ ). Pair-wise comparison showed that the effect of period length for the induction task was much stronger than the application task for both the left and right IPL. This suggests the recruitment of the IPL in rule identification. While *ca vs. sa*, as contrast to *ci vs. si*, mainly activated superior parietal lobule (SPL). The BOLD response of the SPL region is shown in Figure S3 (C, D). Statistical analysis showed that the main effect of period length was significant for both the left SPL ( $F(1, 12) = 9.750, p < 0.01$ ) and the right SPL ( $F(1, 12) = 9.505, p < 0.01$ ), while the interaction effect of task and period length was neither significant. We observed that the BOLD signal of the application task was comparable with that of the induction task, and the effect of period length was also similar for the both tasks. This implies the more important role of the SPL in rule application.

Together, the exploratory analysis has validated our hypothesis of the functional roles of the four ROIs. The exploratory analysis also suggests that rule identification is also associated with the left APFC and the bilateral IPL except the left DLPFC, and rule application is related to the bilateral SPL except the caudate region. However, the goal of this article is try to grasp the main stream of information-processing during inductive reasoning process and would not tend to construct a unified model including all related regions, thus, only the four regions were concerned in this article and the other areas would be discussed in future.

## DISCUSSION

The basic logic in this research is that we can map various components of an information-processing model of inductive reasoning onto various brain regions. According to different functional role of each component, we can postulate their effects of factors in experimental design, thus, we can verify the hypothesis by checking the BOLD response in each region. The basic assumption is that the BOLD response in a particular area reflects only a single postulated cognitive function. As a general assertion this seems

an improbable assumption, but it might be true in specific tasks [31,47]. The main goal of this article is to grasp the main stream of information-processing in inductive reasoning process, thus, it is proper to hold this assumption. The stronger BOLD responses in these ROIs reinforce our beliefs on this. For example, The DLPFC ROI has the maximum BOLD response among all of ROIs and other regions found in the exploratory analysis.

As an empirical summary, this research is largely consistent with existing associations, in the literature, of the fusiform gyrus with visual encoding, the DLPFC with rule identification, the caudate with rule application, and the region of the motor with manual button-pressing. Each of these associations deserves a little comment. First, the fusiform gyrus region locates in the ventral stream of the visual pathway, and associates with object recognition. This article links this area to visual encoding of stimuli is also consistent with [34,48].

Second, our DLPFC focus was found in the left BA 46, which was inferred to be crucial to rule identification. As has been expected, the priming effect in this region does not reach a significant level. Many literatures have suggested the dual-processing mechanism of reasoning [49], *i.e.*, controlled processing and automatic processing. As we know, the priming effect is induced by the automatic processing. We argued that the left DLPFC identified in this study may contribute to both controlled and automatic operations. Additionally, we note that there are other regions which may also participate in rule identification, such as APFC and insula found in the exploratory analysis, although the left DLPFC may play a central role.

Third, we should comment on the association of rule application component with the activation of caudate. The BOLD response in the caudate ROI and exploratory analysis both verified our inference. This is also congruent with the involvement of the caudate in conditional association learning [50], rule-based category learning [51], and rule switching[52]. At last, the manual response has been linked to the activity of the region which includes parts of both the motor and the sensory cortex, along the central sulcus. This has been detailed discussed in previous studies [34].

## CONCLUSION

To our knowledge, this is the first time to relate the information-processing model of inductive reasoning



process to its neural substrates, which is helpful for us to in-depth understand the information-processing mechanism of inductive reasoning process in human brain. The current study links each module to the corresponding region, and verifies these associations by using fMRI data. It is noted that the associations between the four-stage information-processing model of inductive reasoning process and the four ROIs should be judged not as absolutely correct or wrong but rather as more or less fruitful, although one needs to remain mindful of the potential insufficiencies.

## ACKNOWLEDGEMENTS

This work was supported by the Natural Science Foundation of China (Grant Nos. 61105118, 31400958, 61473196), and Open Research Fund of the State Key Laboratory of Cognitive Neuroscience and Learning (No.CNLZD1302).

## SUPPLEMENTARY MATERIALS

The Supplementary materials can be downloaded from the journal website along with the article.

## REFERENCES

- [1] Egan GE, Greeno JG. Theory of rule induction: Knowledge acquired in concept learning, serial pattern learning and problem solving. In L.W. Gregg (Ed.), *Knowledge and cognition*. Potomac, MD: Lawrence Erlbaum Associates Inc. 1974; 43-104.
- [2] Carroll JB. *Human cognitive abilities: A survey of factor-analytic studies*. Cambridge, UK: Cambridge University Press. 1993.
- [3] Csapo B. The development of inductive reasoning: cross-sectional assessments in an educational context. *Int J Behav Dev*. 1997; 20, 609-626.
- [4] Osherson D, Smith E, Wilkie O, Lopez A, Shafir E. Category-based induction. *Psychol Rev*. 1990; 97, 185-200.
- [5] Lin T, Kinshuk, McNab P. Modelling inductive reasoning ability for adaptive virtual learning environment. *Proceedings of the IADIS International Conference on Cognition and Exploratory Learning in Digital Age (CELDA 2004)*, Lisbon, Portugal: IADIS Press 2004; 343-349.
- [6] Goel V, Dolan RJ. Differential involvement of left prefrontal cortex in inductive and deductive reasoning. *Cognition* 2004; 93: B109-B121.
- [7] Liang PP, Zhong N, Wu JL, Lu SF, Liu JM, Yao YY. Time Dissociative Characteristics of Numerical Inductive Reasoning: Behavioral and ERP Evidence. *Proceeding of the International Joint Conference of Neural Network (IJCNN 2007a)*, 873-879.
- [8] Liang PP, Zhong N, Lu SF, Liu JM, Yao YY, Li KC, *et al*. The neural mechanism of human numerical inductive reasoning process: A combined ERP and fMRI study. *LNAI 4845*, Springer 2007b; 223-243.
- [9] Liang PP, Goel V, Jia XQ, Li KC. Different neural systems contribute to semantic bias and conflict detection in the inclusion fallacy task. *Front Hum Neurosci*. 2014a; 8,797.
- [10] Wason PC. Reasoning about a rule. *Q J Exp Psychol*. 1968; 20, 273-281.
- [11] Simon HA, Lea G. Problem solving and rule induction: A unified view. In L.W. Gregg (Ed.), *Knowledge and Cognition*. Hillsdale, NJ: Erlbaum. 1974; 105-127.
- [12] Qin Y, Simon HA. Laboratory replication of scientific discovery processes. *Cogn Sci*. 1990; 14, 281-312.
- [13] Haverty LA, Koedinger KR, Klahr D, Alibali MW. Solving induction problems in mathematics: Not-sotrivial pursuit. *Cogn Sci*. 2000; 24: 249-298.
- [14] Girelli L, Semenza C, Delazer M. Inductive reasoning and implicit memory: evidence from intact and impaired memory systems. *Neuropsychologia* 2004; 42: 926-938.
- [15] Holzman TG, Pellegrino JW, Glaser R. Cognitive variables in series completion. *J Educ Psychol*. 1983; 75: 603-618.
- [16] Lefevre J, Bisanz J. A cognitive analysis of number-series problems: sources of individual differences in performance. *Memory & Cognition* 1986; 14:287-298.
- [17] Delazer M, Girelli L, Benke T. Arithmetic reasoning and implicit memory: a neuropsychological study on amnesia. *Cortex* 1999; 35: 615-627.
- [18] Delazer M, Girelli L. Priming arithmetic reasoning in an amnesic patient. *Brain Cogn*. 2000; 43: 138-143.
- [19] Tulving E, Schacter DL. Priming and human memory systems. *Science* 1990; 247: 301-306.
- [20] Liang PP, Jia XQ, Taatgen NA, Zhong N, Li KC. Different strategies in solving series completion inductive reasoning problems: An fMRI and computational study. *Int J Psychophysiol*. 60.
- [21] Jia XQ, Liang PP, Lu J, Yang YH, Zhong N, Li KC. Common and dissociable neural correlates associated with component processes of inductive reasoning. *Neuroimage* 2011; 56, 2292-2299.
- [22] Jia XQ, Liang PP, Shi L, Wang D, Li KC. Prefrontal and parietal activity is modulated by the rule complexity of inductive reasoning and can be predicted by a cognitive model. *Neuropsychologia* 2015; 66:67-74.
- [23] Xiao F, Li P, Long CQ, Lei Y, Li H. Relational complexity modules activity in the prefrontal cortex during numerical inductive reasoning: An fMRI study. *Biol Psychol* 2014; 101:61-68.
- [24] Zhong N, Liang PP, Qin YL, Lu SF, Yang YH, Li KC. Neural substrates of data-driven scientific discovery: An fMRI study during performance of number series completion task. *Science in China Series C: Life Sci*. 2011; 54(5): 466-473.
- [25] Yang YH, Liang PP, Lu SF, Li KC, Zhong N. The role of the DLPFC in inductive reasoning of MCI patients and normal agings: An fMRI study. *Science in China Series C: Life Sci*. 2009; 52(8): 789-795.
- [26] Sternberg RJ. *Intelligence, information processing and analogical reasoning: The component analysis of human ability*. Hillsdale, NJ: Lawrence Erlbaum Associates Inc. 1977.
- [27] Sternberg RJ. Toward a unified theory of human reasoning. *Intelligence* 1986; 10, 281-314.
- [28] Klauer KJ. A process theory of inductive reasoning tested by the teaching of domainspecific thinking strategies. *Eur J Psychol Educ*, 1990; 5, 191-206.
- [29] Klauer KJ. Teaching inductive reasoning: some theory and three experimental studies. *Learning and Instruction* 1996; 6, 37-37.
- [30] Anderson JR. ACT: A simple theory of complex cognition. *Am Psychol*. 1996; 51, 355-365.
- [31] Anderson JR, Qin Y, Stenger VA, Carter CS. The relationship of three cortical regions to an information-processing model. *Cogn Neurosci*. 2004; 16, 637-653.
- [32] Anderson JR, Fincham JM, Qin Y, Stocco A. A central circuit of the mind. *Trends Cogn Sci*. 2007; 12, 136-143.

- [33] Qin Y, Bothell D, Anderson JR. ACT-R meets fMRI. *LNAI* 4845, Springer, 2007; 205-222.
- [34] Anderson JR, Qin Y. Using brain imaging to extract the structure of complex events at the rational time band. *J Cogn Neurosci*. 2008; 20, 1624-1636.
- [35] Christoff K, Prabhakaran V, Dorfman J, Zhao Z, Kroger JK, Holyoak KJ, Gabrieli JDE. Rostrolateral prefrontal cortex involvement in relational integration during reasoning. *NeuroImage*, 2001; 14, 1136-1149.
- [36] Osherson D, Perani D, Cappa S, Schnur T, Grassi F, Fazio F. Distinct brain loci in deductive versus probabilistic reasoning. *Neuropsychologia* 1998; 36, 369-376.
- [37] Prabhakaran V, Smith JAL, Desmond JE, Glover GH, Gabrieli JDE. Neural substrates of fluid reasoning: an fMRI study of neocortical activation during performance of the Raven's Progressive Matrices Test. *Cogn Psychol*. 1997; 33, 43-63.
- [38] Stocco A, Anderson JR. Endogenous control and task representation: an fMRI study in algebraic problem solving. *J Cogn Neurosci*. 2008; 20, 1300-1314.
- [39] D'Esposito M, Detre JA, Alsop DC, Shin RK, Atlas S, Grossman M. The neural basis of the central executive of working memory. *Nature* 1995; 378, 279-281.
- [40] Fincham JM, Anderson JR. Distinct roles of the anterior cingulate and prefrontal cortex in the acquisition and performance of a cognitive skill. *Proc Natl Acad Sci U S A*. 2006; 103, 12941-12946.
- [41] Chochon F, Cohen L, Moortele PF, Dehaene S. Differential contributions of the left and right inferior parietal lobules to number processing. *J Cogn Neurosci*. 1999; 11, 617-630.
- [42] Sandrini M, Rossini PM, Miniussi C. The differential involvement of inferior parietal lobule in number comparison: a rTMS study. *Neuropsychologia* 2004; 42, 1902-1909.
- [43] Bamiou D, Musiek FE, Luxon LM. The insula (Island of Reil) and its role in auditory processing: Literature review. *Brain Res Rev*. 2003; 42, 143-154.
- [44] Chee MWL, Soon CS, Lee HL, Pallier C. Left insula activation: a marker for language attainment in bilinguals. *Proc Natl Acad Sci U S A*, 2004; 101, 15265-15270.
- [45] Christoff K, Ream JM, Geddes LPT, Gabrieli JDE. Evaluating self-generated information: anterior prefrontal contributions to human cognition. *Behav Neurosci*. 2003; 117, 1161-1168.
- [46] Strange BA, Henson RNA, Friston KJ, Dolan RJ. Anterior prefrontal cortex mediates rule learning in humans. *Cereb Cortex* 2001; 11, 1040-1046.
- [47] Anderson JR, Fincham JM. Extending problem-solving procedures through reflection. *Cogn Psychol*. 2014; 74:1-34.
- [48] McCandliss BD, Cohen L, Dehaene S. The visual word form area: expertise for reading in the fusiform gyrus. *Trends Cogn Sci*. 2003; 7, 293-299.
- [49] Evans JSBT. In two minds: dual-process account of reasoning. *Trends Cogn Sci*. 2003; 7, 454-459.
- [50] Pasupathy A, Miller EK. Different time courses of learning related activity in the prefrontal cortex and striatum. *Nature* 2005; 433, 873-876.
- [51] Filoteo JV, Maddox WT, Simmons AN, David A, Cagigas XE, Matthews S, Paulus MP. Cortical and subcortical brain regions involved in rule-based category learning. *Neuroreport* 2005; 16, 111-115.
- [52] Vervy SP, Brown GG, Frank L, Paulus MP. Error-rate-related caudate and parietal cortex activation during decision making. *Neuroreport* 2003; 14, 923-928.

Received on 14-11-2014

Accepted on 03-12-2014

Published on 14-04-2015

<http://dx.doi.org/10.15379/2409-3564.2015.02.01.2>

© 2015 Jia and Liang; Licensee Cosmos Scholars Publishing House.

This is an open access article licensed under the terms of the Creative Commons Attribution Non-Commercial License

(<http://creativecommons.org/licenses/by-nc/3.0/>), which permits unrestricted, non-commercial use, distribution and reproduction in any medium, provided the work is properly cited.